Minimax Theory and its Applications
Volume 11 (2026), No. 4s, 978-989

AI-Driven Models for Forecasting Black Sigatoka Progression in Banana Foliage

Dr. V K Senthil Ragavan[1*], Dr. Nor Asilah Wati Abdul Hamid[2], Dr. Dafik[3], Dr. R. Sunder[4], Dr.Siva Shankar Subramanian[5]

[1*]Professor, Department of CSE, Sri Shanmugha College of Engineering and Technology, Sankari, Salem(D.T.), Tamil Nadu– 637 304, India, Email: vksenrag@yahoo.com, Orcid : 0000000185733040
[2]Associate Professor, Institute for Mathematical Research, Universiti Putra, Malaysia, 43400 UPM Serdang, Selangor, Malaysia, Email: asila@upm.edu.my
[3]Combinatorics, Graph theory and Network Topology Research Group (CGANT), University of Jember, Jember, Jawa Timur 68121, Email: d.dafik@unej.ac.id
[4]Professor, School of Computer Science and Engineering, Galgotias University, Uttar Pradesh, India - 203201. Email: sunder.r@galgotiasuniversity.edu.in
[5]Professor & Head IPR, Department of CSE, KG Reddy College of Engineering and Technology, Hyderabad,Telangana, India – 501504, Email: drsivashankars@gmail.com, https://orcid.org/0000-0002-7616-6088

Abstract
Banana plantations play an important role in the agricultural sector of the world and the diseases like the Black Sigatoka which is brought about by the Mycosphaerellafijiensis (Mf) can have a drastic impact to the crop production. Such diseases need to be diagnosed timely and correctly in order to be effectively controlled and treated to avoid huge losses and offer a reliable source. The study combines two sophisticated methods, which include contour mathematics and Deep Extreme Learning Machines (D-ELM). Banana leaf pattern and detailing are studied with the help of contour mathematics. It is a necessary analysis as it leads to defining the slight alterations in the shape of the leaf signifying the initial phases of disease infestation. Early intervention then becomes essential to check the disease before it becomes large scale. D-ELM is an advanced form of machine learning that displays superior results and high accuracy when it comes to handling large datasets. This is a component of the study that is necessary in the successful management of large volumes of data (which are frequently applied) during agricultural experiments to maintain accuracy and reliability of predictions. D-ELM algorithm is trained with a set of diseased and healthy banana leaves images. Such a model, especially its speed and accuracy is far greater than that of the traditional system of detecting disease.Further on, the fact that over 95% accuracy in accurately predicting plant disease is great. Besides the fact that the early detection of Black Sigatoka has high credibility, the same degree of precision is an innovative benchmark to be used in the future studies. Proper and timely identification at the early stages enables proper and timely interventions that will not allow the disease to inflict much harm. Not only does the accuracy of the method increase confidence in early detection, but it also creates a new benchmark of the following research on the disease control in banana cultivation through the advanced AI techniques.

Keywords*:* deep learning, disease detection, banana farming, black sigatoka, accuracy, classification, preprocessing,

1. Introduction

Technological advancements have continued to have a significant impact on many facets of society in recent years. In medicine, for instance, early self-health diagnostic tools have been created and are already in use, and online commerce has flourished globally. The agricultural industry is also not left behind. Many efforts have been made to implement technology in the agricultural industry [1]. A multitude of issues, including diseases like Black Sigatoka, which is allegedly a danger to world food security, require technology to be addressed. Mycosphaerellafijiensis is the causative agent of this fungal illness. Plantains and banana leaves are both impacted by this fungus (1). Farmers' economies around the world are impacted, and things are especially difficult in poor nations like Tanzania. About 40 million Tanzanians, or 60% of the country's population, make their living from agriculture (2). Their economic stability and food security may be significantly impacted by the catastrophic effects of Black Sigatoka sickness [2-4].

When a plant's capacity for photosynthesis is compromised by the Black Sigatoka fungus, it is unable to generate the necessary quantity of food, which can lead to the plant dying or producing lower-quality fruits [5]. Early on, the condition is characterized by faint brown streaks that eventually develop into distinct black patches. The first phases are typically exceedingly hard to identify, as previous studies have also shown. One such study was conducted by (3), which attempted to address the issue by creating an automated approach for

early diagnosis [6]. Different stages of the disease have been proposed by studies.Some suggested six stages, but others suggested changing the six to four stages of the illness depending on the severity of the infection. The disease's stages are categorized using the phrases "high," "medium," "early," and "health" [7-9].
As previously mentioned, technology has remained a significant factor in solving issues in a variety of industries, including agriculture. Artificial intelligence has become more and more prevalent in recent years, offering a variety of options. In a variety of industries, deep learning has proven effective in handling classification jobs [10, 11]. Various algorithms have been used in various research. With the use of images, convolutional neural networks (CNN) have demonstrated encouraging outcomes in the early detection and precise classification of diseases.For instance, the work by [12] used the ShuffleNet V2 algorithm, which is a CNN architectural version, and contrasted it with other machine learning architectures, particularly K-Nearest Neighbour (KNN) and Support Vector Machine (SVM). In an effort to overcome the difficulties posed by Black Sigatoka, [13] developed models to identify diseased banana leaves using hyperspectral pictures. Mobile technology has been used by other investigations, as those by [14, 15] , to implement their categorization methods.Figure 1 depicts the six phases of the Black Sigatoka invasion of banana leaves.



Figure 1. Six phases of the Black Sigatoka invasion of banana leaves. (1) Early Infection, (2) Progression, (3) Intermediate Stage, (4) Advanced Infection, (5) Severe Infection and (6) Late Stage

Nevertheless, the illness still exists despite these noted remedies. It is evident that the important task of categorizing Black Sigatoka disease according to its stages of advancement has not been explored in many of the research that have been conducted. The possibility to effectively manage the disease at its various stages and provide the necessary intervention techniques at each particular stage is presented by addressing the issue via its stages of advancement (10). The majority of the literature ignores the progression from early signs to severe infection in favor of classifying people as either infected or healthy. The goal of our research is to close this information gap.
The key contribution of this research are as follows,

- To establish an effective framework for early disease detection in banana plantations by integrating contour mathematics with Deep Extreme Learning Machines (D-ELM).
- The use of contour mathematics enables detailed analysis of leaf shape variations, allowing identification of early-stage Black Sigatoka infection.
- For handling large-scale agricultural image datasets efficiently, the D-ELM algorithm provides superior speed, precision, and reliability compared to conventional methods.
- The proposed method sets a new benchmark for precision-driven plant disease detection, contributing significantly to sustainable banana farming practices.
-

Table 1. An exhaustive review of the fundamental elements of Black Sigatoka conditions affecting banana leaves.

Characteristic	Overview
Causal Organism	Ascomycete fungus (Mycosphaerellafijiensis)

Symptom Stages	1. Early Infection	Small, 1 mm diameter yellowish dots on the underside of the leaf
	2. Progression	Brown or red streaks measuring 1 to 5 millimetres
	3. Intermediate Stage	Streaks that resemble stage 2 but are longer than 5 mm
	4. Advanced Infection	The abaxial leaf surface exhibits brown elliptical stripes, whereas the adaxial leaf surface displays black streaks.
	5. Severe Infection	The streaks seem completely black and extend to the lower surface of the leaf, with a yellow halo around them.
	6. Late Stage	The centre of the streak is a light grey colour, encircled by a black ring and a yellow halo.
Lesion Size		expanding up to several centimeters; 1-6 mm initially
Lesion Shape		Streak-like or Elliptical
Lesion Color		Starts light yellowish or brown, turns darker (black) as it matures
Leaf Impact		Reducing photosynthetic area, premature leaf necrosis
Disease Progression		Rapid; can defoliate plants within 6-8 weeks under high humidity and temperature
Optimal Conditions		Warm temperatures (between 22 to 28°C), high humidity (> 90%)
Spore Production		Prolific; producing numerous spores that are easily dispersed by wind
Management Strategies		Resistant cultivars,fungicide application, cultural practices (e.g., pruning, sanitation)

2. Related Work

Sujatha et al. [11] evaluated several datasets, including banana leaves, and combined deep learning (DL) and machine learning (ML) approaches for plant leaf disease identification. For the banana leaf dataset, their approach, which fused Inception v3 and SVM, produced an accuracy of 91.9%, proving the usefulness of hybrid ML-DL frameworks for certain crop diseases.

Mora et al. [12] also introduced a georeferenced surveillance system of banana wilt illnesses, a hybrid of human-in-the-loop AI approaches and multiple YOLO foundation models. Their system showed that explainable AI is important to have a reliable and scalable disease surveillance system because it could achieve good precision and recall in diverse geographic areas.

To classify plant diseases, Batool et al. [13] have developed a lightweight deep learning model which integrates depthwise separable convolutions and spatial attention. This method was very efficient and could be applied in resource-limited agricultural contexts with an accuracy of 98.7 percent on the PlantVillage dataset.

Lastly, Bagheri and Kafashan [14] implemented UAV-based remote sensing to present an in-depth evaluation of the vegetation indices and data processing methods of monitoring orchards. Their study contributes valuable information regarding the selection of the most appropriate indices, data processing methods, and the assessment of the diseases and decision making in orchard crops, including banana plantation.

3. Meterials And Methods

3.1. Data Collection

The photos of Black Sigatoka in this study were taken in a publicly available database. The dataset has 16,092 images of banana leaves and stems making it the largest publicly available collection of photos related to bananas in Tanzania. The database photographs were collected in various Tanzanian farms of the selected places. These regions are; Kilimanjaro, Mbeya, Arusha, Dar es Salaam and Kigera. These regions were chosen depending on the volume of bananas grown and prevalence of the disease. These were captured using the mobile phones.The agricultural experts were employed to provide the required supervision. In this investigation, images of the healthy and Black Sigatoka-infected banana leaves were obtained in the dataset. After completion of the first phase of preprocessing, that is, removal of duplications, 5767 pictures of Black Sigatoka were left. All the photos contained in the dataset were jpeg format and were 1024 x 768 pixel in size. As per the name of the classes, all the pictures were named according to a number format within a specific sub-directory. It is important to note that the photos taken by the Black Sigatoka did not belong to this collection as it was the photos categorized by their stages of infection. The researcher had to work closely with three agriculture professionals to divide the photos into their respective group stages.

3.2. Preprocessing

Before training any model, it is important that the data is first preprocessed. The data obtained were not in format and forms that could be used as intended. To preprocess the data to be used in this investigation, the following tasks were done:

The pictures that were collected in the different locations had a resolution of 1024 x 768 pixels. In some jobs this image quality is considered good however in others not. The photos would need additional resources when developing the models and this would translate into poor performance of the model. In order to make the model more effective on the whole, the photos should be enlarged. Research has also pointed out that poor image scaling may lead to poor results of deep neural network models and therefore appropriate methods are to be considered when scaling down the photographs. Moreover, it has been proved that despite a smaller size of images, it is possible to use the scaled versions of the image, and the models can still work reasonably well

without affecting the precision of the results. As such, this reduces the complexity of the model, without deteriorating its performance. The photos, which were used in the experiments carried to conduct this study, were reduced to 224x224 pixels. With the desire to achieve greater model accuracy, it is said that there is no universal size of an image and it is a matter of trial and error.

Using various transformations or modification approaches, data augmentation entails producing new data from the existing data. Examples of transformation are rotation, cropping, shear, flipping, scaling, and many others. The dataset's photos of BlackSigatoka-infected banana leaves were not originally gathered with the intention of classifying them according to their phases. A data imbalance was noticed during the process of classifying them into their corresponding stages; there were more pictures of Black Sigatoka-infected leaves in the advanced and intermediate stages than in the early stages. Therefore, a Python augmentation package was used to perform rotation, flipping, shearing, and cropping modifications in order to overcome this difficulty.

CLAHE (Contrast LimitedAdaptive Histogram Equalization) (Reza, 2004) is an established approach applied to improve the image contrast, particularly in regions with a low contrast. It's a more sophisticated conventional Adaptive Histogram Equalization (AHE) that limits contrast amplification to minimize noise amplification. CLAHE shines in fields like medical imaging and agriculture, where it could boost the characteristics of banana leaf images to identify Mycosphaerellafijiensis diseases.Once the region contrast are enhanced, grayscale image I of size $M \times N$ are divided$I$ into non-overlapping contextual regions (tiles) of size $X \times Y$. Typically, X and Y are much smaller than M and N.

For each kth tile, the histogram h_k is computed. Further, to perform contrast limiting L, a predefined limit is fixed as a threshold to clip/trim the surplus and evenly divide it across all bins. The next process is to compute the cumulative distributive function for each clipped histogram, which is expressed as,

$$\boldsymbol{f_k(i) = \sum_{j=0}^{i} h_k(j)} \quad \textbf{(1)}$$

where $f_k$is always normalized to have high value of 255.

The subsequent stage entails using bilinear interpolation, a technique employed on the equalized values of these individual tiles. This interpolation method approximates the value of $p(x,y)$ by calculating a linear combination of the values in the four adjacent tiles. Thus, for each pixel $p(x,y)$ in the actual image, four tiles surrounding $p$is identified and bilinear interpolation is performed using the equalized values from the$p$, which is computed as,

$$\boldsymbol{I_{new}(x,y) = inp\left(x,y,f_{top-left},f_{bottom-left},f_{top-right},f_{top-right}\right)} \quad \textbf{(2)}$$

It is an effective method of helping the smooth transition between different areas of the image, maintaining its natural look yet enhancing the contrast and degree of detail.

Once interpolation is done, the initial pixel value at the point (x,y) will be replaced with the interpolated value that has been estimated. The process is repeated on the entire image, hence enhancing every pixel of the image to a better version. After all the pixels have been processed, the image is recreated. The altered tiles are combined together to form a new and improvedimageInew. The image is improved with increased clarity of such significant features as the distinction of texture and accurate detail of dots or spots on the banana leaves.

The final and the most important step of this procedure is the application of contour detection methods, including the Canny Edge Detection (CED) approach (Song et al., 2017). The algorithm is very good in precisely identifying the actual edges of the leaves and any other prominent features that may be on the leaves like areas that have been affected by illness. With the help of CED on the enhanced image, we are able to draw the lines of the leaf outlines and any anomalies which exist accurately. This is very instrumental in the effective identification and diagnosis of diseases like Mycosphaerellafijiensis infestation. A combination of CLAHE and advanced contour detection is incredibly effective at providing early and accurate disease diagnosis in banana leaves, which can be used to learn better how agricultural management can be conducted.

3.3. Contour Mathematics

The mathematical computations of enhanced procedures of the CED process are illustrated in Table 2.

Table 2. Enhanced CED algorithm

Input: $I_{new} \rightarrow I_{eq}$ *//set of equalized images* *Output:* $\mathscr{E}_{merge}$ *//combined edges*
For each scale σ in scales ɖ: $I_\sigma = I_{eq} * G_\sigma$ *//applying Gaussian blurs* Compute gradients: $G_x = \frac{\partial I_\sigma}{\partial x}, G_y = \frac{\partial I_\sigma}{\partial y}$ $M_\sigma = \sqrt{(G_x^2) + (G_y^2)}$ *//gradient magnitude* $\Phi_\sigma = arctan\left[{}^{G_y}\!/_{G_x}\right]$ *//gradient direction* $q_\sigma = C_\sigma^F * M_\sigma$ *//applying custom filter to each scale*

//based on the characteristics of I, $\mathcal{T}$ is determined

$N_\sigma = NMS[q_\sigma, \Phi_\sigma]$ *//non-maximum suppression*

$\mathscr{E}_\sigma = hysteresis[N_\sigma, \mathcal{T}_{low}, \mathcal{T}_{high}]$ *//edge tracking by hysteresis*

$\mathscr{E} = \cup_{\sigma \in \mathcal{Q}} \mathscr{E}_\sigma$ *//merging multi-scale edges*

For each channel, $\mathbb{C} \in \{R, G, B\}$:

$\mathscr{E}_{\mathbb{C}} = enhancedCanny(I_{\mathbb{C}})$

$\mathscr{E}_{merge} = \{\mathscr{E}_R \cup \mathscr{E}_G \cup \mathscr{E}_B\}$ *//merging color channel edges*

Feature Extraction

The Gray-Level Co-Occurrence Matrix (GLCM) characteristics have been retrieved for this research.

GLCM

The GLCM feature takes advantage of the unique bond among two pixels in an image that are separated by a specific distance. In areas with fine texture, the GLCM feature's value changes quickly, while in areas with coarse texture, it changes more slowly. It is calculated as

$$\boldsymbol{GLCM(i,j)} = \sum_{(x,y)} \begin{cases} \mathbf{1}, & if\ I(\boldsymbol{x},\boldsymbol{y}) = \boldsymbol{i} and\ I(\boldsymbol{x}+\Delta\boldsymbol{y}+\Delta\boldsymbol{x},\boldsymbol{y}) = \boldsymbol{j} \\ \mathbf{0}, & \boldsymbol{otherwise} \end{cases} \quad \textbf{(3)}$$

The GLCM matrix is created for the full image utilizing this method. Next, this GLCM matrix is divided into n ~ n non-overlapping blocks. Statistical characteristics such as correlation, contrast, entropy, energy, homogeneity, and angular second moment were retrieved for every block.

Angular second moment:

The picture distribution's homogeneity is represented by the angular second moment. It is calculated as

$$A_{sm} = \sum_{m=1}^{M} \sum_{n=1}^{N} G(m,n)^2 \quad (4)$$

Correlation: The correlation value shows how similar the image's texture is in the horizontal and vertical dimensions, which are perpendicular. It is calculated using

$$C = \frac{\sum_{m=1}^{M} \sum_{n=1}^{N} (m-x)(n-y)G(m,n)}{\sigma_x \sigma_y} \quad (5)$$

Contrast: The contrast value is calculated as follows and shows how the image's smooth areas and depth vary:

$$C_{on} = \sum_{m=1}^{M} \sum_{n=1}^{N} (m-n)^2\, G(m,n) \quad (6)$$

Entropy: This metric, which quantifies the amount of information present, is calculated using

$$E_{nt} = -\sum_{m=1}^{M} \sum_{n=1}^{N} G(m,n) I_g G(m,n) \quad (7)$$

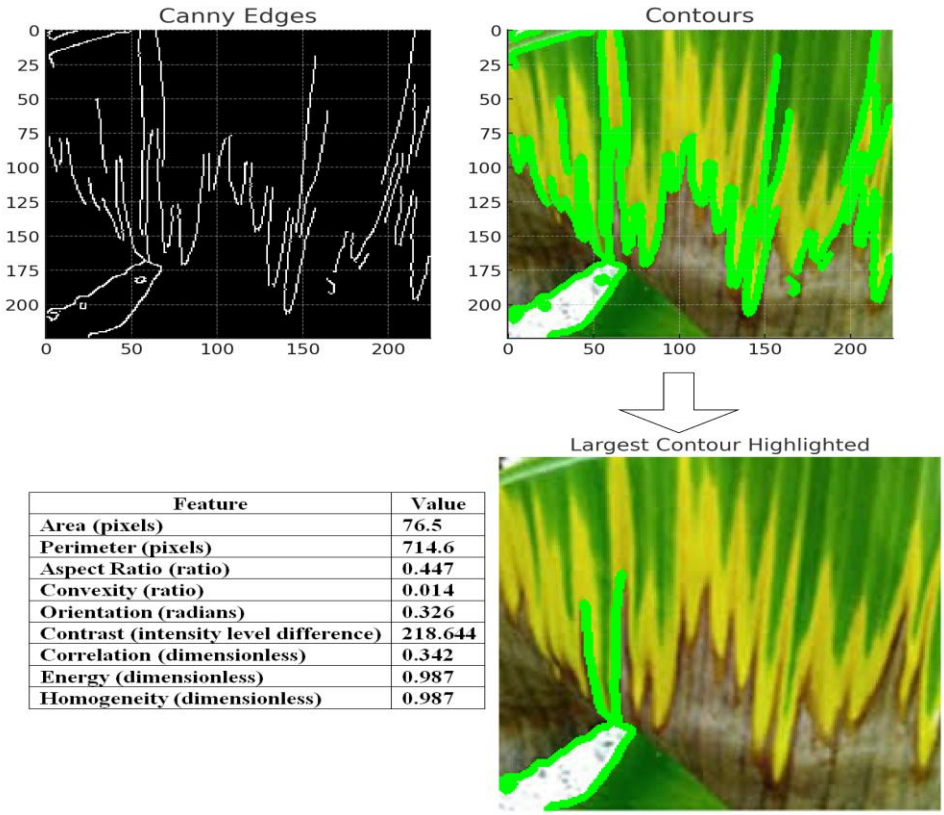

Feature	Value
Area (pixels)	76.5
Perimeter (pixels)	714.6
Aspect Ratio (ratio)	0.447
Convexity (ratio)	0.014
Orientation (radians)	0.326
Contrast (intensity level difference)	218.644
Correlation (dimensionless)	0.342
Energy (dimensionless)	0.987
Homogeneity (dimensionless)	0.987

Figure 2. Sample Outcome of the Preprocessing Phase

The sample result of the preprocessing step is outlined in Figure 2; it can be seen that the RoI has been successfully delineated on the banana leaf picture. This area is the most salient one to which the analysis will be focused on. The geometric and textural features of this particular RoI have been carefully measured: The area is 76.5 pixels, and the perimeter is 714.6 pixels. The aspect ratio has been determined to be 0.447 that shows the width to height ratio. The convexity of 0.014 and the angular direction of the contour of 0.326 radians are the computed angle of the convex hull and the angular direction of the contour.

Additional analysis of the textures using the GLCM has produced some worthwhile results: The contrast is 218.644 which implies that there is a significant difference in intensity between neighboring pixels. The correlation is 0.342 and this represents the extent to which a pixel is similar to its neighbor, thus, determining texture uniformity. The energy, a summary statistic of the GLCM, is great, 0.987 meaning uniformity in the textures, and the homogeneity, 0.987, is also high, meaning that the GLCM has a small variation, a factor that demonstrates smoothness of the texture of the highlighted RoI. These numerical measures are a strong basis of additional inspection and examination of the health of the banana leaf.

4. D-ELM SETUP

In spite of the benefits of ELM in certain applications, where rapid training is an important attribute, particularly where dealing with a large dataset, the effect of this is frequently a reduced ability to refine the model based on the training data, which is a characteristic of the traditional neural network (NN), using backpropagation. In order to deal with this limitation, we combined D-ELM with numerous stacks (layers), which were then followed by a non-linear activation function. This allows the establishment of a deeper architecture that can obtain more complex representational procedures as shown in Figure 3.

To implement a D-ELM, multiple layers are arranged, each layer has the output of the previous layer, which has a non-linear transformation and is inputted to the next layer. The architecture helps acquire more complex patterns in data. The next computation constitutes the salient processes of D-ELM.



Figure 3. D-ELM Process

4.1. Initialization

Initialization of each of the layers in a D-ELM model is performed by randomly selecting input weights (w i) and biases (e i). Randomization process is an inherent quality of D-ELMs, which distinguishes them among traditional NNs which usually initialize those weights with pre-training or some other heuristic. Subsequently, a non-linear activation operation, represented as $A(\cdot)$, is determined for each neuron in the layer. Typical options for this kind of function consist of the sigmoid function. Still, we opted for the Rectified Linear Unit (ReLU) function (Agarap, 2018), which is preferred for its capability to minimize the occurrence of disappearing gradients throughout training. The D-ELM layer is built around a blend of non-linear activation functions and random weight initialization, which is the basis for the following learning process.

4.2. Forward Pass

The determinationof hidden layer output(h_i)for each D-ELM layer (L_i) and each input I is computed as,

$$\boldsymbol{h_i = A(I \times \omega_i) + e_i} \quad \textbf{(8)}$$

Equation (5) illustrates that the resultant of the h_i is utilized as I for the subsequent layer L_{i+1}.

1. t Weight Calculation

ute the output weights β for the ultimate ELM layer L_n, it is essential to compute the least squares issue.

$$\boldsymbol{\beta = h_n^{\dagger} T} \quad \textbf{(9)}$$

where $h_n^{\dagger}$ indicates the Moore-Penrose generalized inverse of the hidden layer output matrix h_n, and Tdenotes the target output matrix.

The entire model is trained based on the performance of the forward pass over all layers of the D-ELM network. Later, the final output weight β is computed for the last layer using the same output weight estimation technique.

4.3. Model Training

The complete model is trained based on the performance of the forward pass over all layers of the D-ELM network. Later, the final output weight β is computed for the L_n using the same output weight estimation technique.

4.4. Prediction

To process a new input I_{new}, the network performs a forward pass to determine the final hidden layer output h_{new}. Subsequently, the predicted output P_{new} is determined.

$$\boldsymbol{P_{new} = h_{new}\beta} \quad \textbf{(10)}$$

It is customary to adjust the least-squares resolution through the addition of a regularization term to include regularization in the computation of the output weights in a D-ELM. Ridge regression, commonly called Tikhonov regularization, is a common approach for addressing this issue. The procedure for computing the β with regularization is as follows:

$$\boldsymbol{\beta = h^T T(h^T h_M + I_M \lambda)} \quad \textbf{(11)}$$

From equation (8) h_M indicate the hidden layer's output matrix, h^T represents the transpose, λ denote the regularization attribute, and I_M projects the identity matrix.The inclusion of the regularization term λ in the final result prevents excessive reliance on the specific characteristics of the training data, hence mitigating overfitting.

5. Model Evaluation And Analysis

The proposed model will need an effective arrangement that is practical and has a large capacity of processing as well as good skills in data management. The software environment supports multiple processing at a given time and also has an advanced library of matrix operations. Table 3 shows a detailed examination of the key hyperparameters, software architecture and the version that was necessary to develop and test D-ELM that was used to forecast the presence of Mycosphaerellafijiensis infection on banana leaves.

Table 3. Empirical Specifications

Requirement	**Essential Versions**
Parallel Processing Support	Multi-threading capability in CPUs, Support in software framework
Matrix Computation Libraries	NumPy v1.20, SciPy v1.6 for Python
ML Framework	TensorFlowv2.4, PyTorchv1.7
GPU Acceleration	CUDA-enabled GPUs, cuDNN library support
Hyperparameter	**Range/Values**
Number of Hidden Layers	3 layers
Nodes in Each Hidden Layer	500 nodes per layer
Activation Function	ReLU (Rectified Linear Unit)
Regularization Parameter (λ)	0.001
Optimizer	ADAM (Zhang, 2018)
Input Weight Initialization	Random Initialization
Bias Initialization	Initialized to small random values
Learning Rate (for output layer)	0.01
Loss Function	Mean Squared Error (MSE)

Output Layer Weight Initialization	He Initialization
Batch Size	64
Training Epochs	20

The following five performance indicators (Table 4) were used to determine the effectiveness of D-ELMs in predictive modeling, and more specifically, predict plant diseases, including Mycosphaerellafijiensis infestation in banana leaves. Also, they are used to compare D-ELM with other deep learning models, such as BananaSqueezeNet, LeNet, InceptionNet-V3 (Bhuiyan et al., 2023) and ResNet-50 (Yan et al., 2023).

Table 4. Evaluation Metrics

Performance Indicators	**Computations** (Sokolova et al., 2006)
Accuracy	$\frac{\text{Number of correct predictions}}{\text{Total number of predictions}}$
Precision	$\frac{\text{True Positives (TP)}}{\text{TP + False Positives (FP)}}$
Sensitivity	$\frac{\text{True Positives (TP)}}{\text{TP + False Negetive (FN)}}$
F-Score	$2 \times \frac{\text{Precision} \times \text{Sensitivity}}{\text{Precision} + \text{Sensitivity}}$
Area Under Curve (AUC)	The AUC metric comprehensively evaluates the model's performance across all potential categorization levels. A more significant AUC value indicates superior performance of the model.

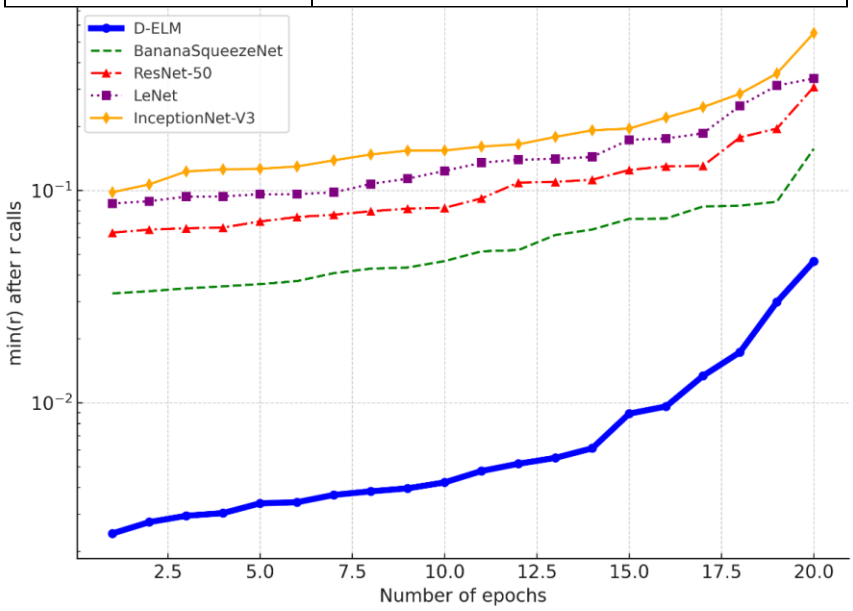

Figure 4. Convergence Analysis Curve

Figure 4 presents a curve of convergence analysis that compares the effectiveness of D-ELM with different models such as BananaSqueezeNet, ResNet-50, LeNet and InceptionNet-V3 on different epochs. min(r) denotes the smallest or the least value of a performance indicator (error rate) that has been calculated and obtained so far and is at the rth iteration. The convergence plot (plotted as a logarithmic plot) of the results obtained by the min(r) after r calls on the y-axis is an effective way of demonstrating how models are progressing as well as their efficiency over a time period, during training. The rapid learning is indicated by a sharp decline. Meanwhile, horizontal trend suggests that the model has already attained the state of stability and does not improve significantly with additional training. This can regularly be employed to track the optimum performance of the model through the training period. The results prove that the proposed D-ELM strategy attains a stable minimum at the initial stages and maintains this low level on the way. Concurrently, the other strategies are either slower in converging or they reach a plateau at a greater level of the performance parameter. To be more exact, the D-ELM levels off with a value that is under 0.1 on the logarithmic scale, whereas other models like BananaSqueezerNet and ResNet-50 stagnate at approximately 0.2 and 0.3, respectively. The plot

describes the amazing efficiency and the precision of D-ELM in the process of training where a strong model is portrayed that is able to predict the required outcome with a lot of precision using fewer epochs. This plays a vital role in practice by monitoring and controlling the condition of plants.

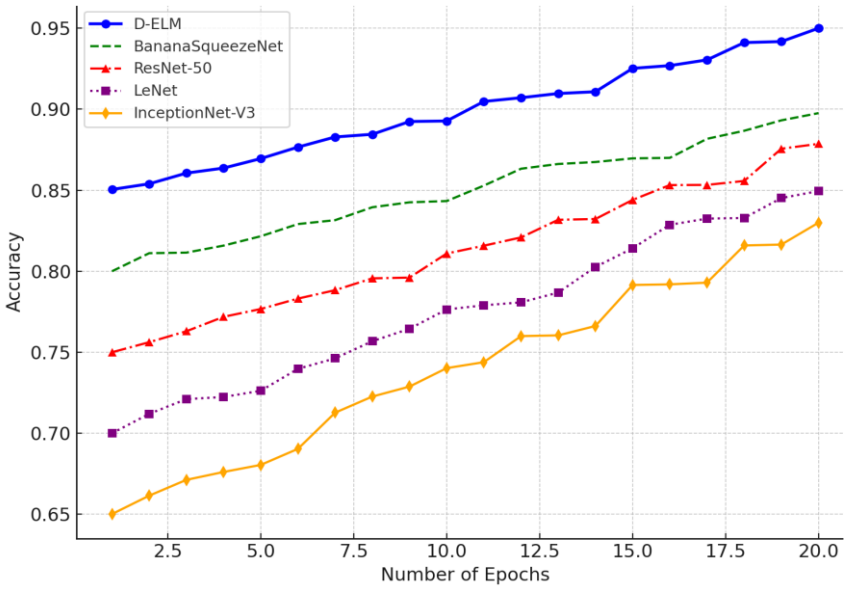

Figure 5. Accuracy Comparison over Epochs

Figure 5 compares the accuracy of five distinct DL models.

Table 5. Sensitivity and F1-Score Evaluation

Model	Sensitivity	F1-score
D-ELM	0.93±0.03	0.92±0.01
BananaSqueezeNet	0.85±0.05	0.81±0.02
ResNet-50	0.83±0.04	0.79±0.02
LeNet	0.78±0.04	0.75±0.02
InceptionNet-V3	0.75±0.05	0.72±0.03

Table 5 is an outcome of the comparison of the performance of some of the DL approaches. In their turn, the rest of the models, i.e., BananaSqueegeNet, ResNet-50, LeNet, and InceptionNet-V3, are less sensitive and have a lower F1-score, with a more significant number of variations. This implies that they need to work on the issue of frequent observation of infected leaves and balancing the trade-off between the accuracy and the memory. An advantage of using D-ELM model over the rest is that it is more sensitive and has high F1 score when it comes to identification of Mycosphaerellafijiensis. This would be essential because false negative may result in unregulated growth of the disease.

The graph of the rate of true positives (TPR) versus the rate of false positives (FPR) (Figure 6) demonstrates the knowledge of the ability of the models to distinguish the infected and healthy leaves.The suggested D-ELM model is located at the upper-left corner, which is a high TPR and a low FPR. It will therefore have a maximum AUC of 0.981. This has admirable efficiency in that the model correctly classifies most of the infected leaves, and minimizes the misclassification of healthy leaves. BananaSqueezerNet is performing well, the TPR is high, and FPR is low, and the AUC can be 0.952. The ResNet-50 and the LeNet show significantly less efficiency with the values of AUC of 0.941 and 0.925, respectively. These models are good in terms of discriminative capability though they are not as effective as the D-ELM. Next, InceptionNet-V3 is expected to have an AUC of approximately 0.90. This suggests that it performs less effectively across the outlined models, but it is still substantially better than arbitrary speculation. The D-ELM approach generally provides the most efficient method for predicting MycosphaerellaFijiensis infection, with the rest of the models performed in decreasing order of effectiveness. The robust AUC values obtained from all models indicate that DL is a feasible tool for this purpose, with D-ELM showing the highest potential for practical use in farming disease control.

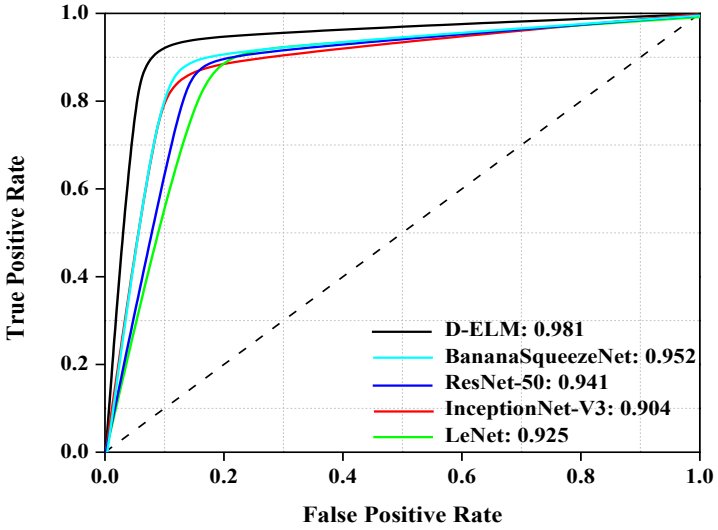

Figure 6. Comparative AUC Curve Analysis

The confusion matrices of all models are presented in table 7, as heatmaps. Each of the matrices provides useful data on how the model can segment the cases into the categories of class 0 (productive leaves) or class 1 (infected leaves). The lower-right and upper-left cells of every matrix show the number of successful classifications (True Positives and True Negatives, respectively). Conversely, the misclassifications are shown in the lower-left and upper-right cells (False Negatives and False Positives, respectively).
D-ELM model shows numerous True positives and negatives indicating strict classifications with minimal instances of false positives and false negatives.

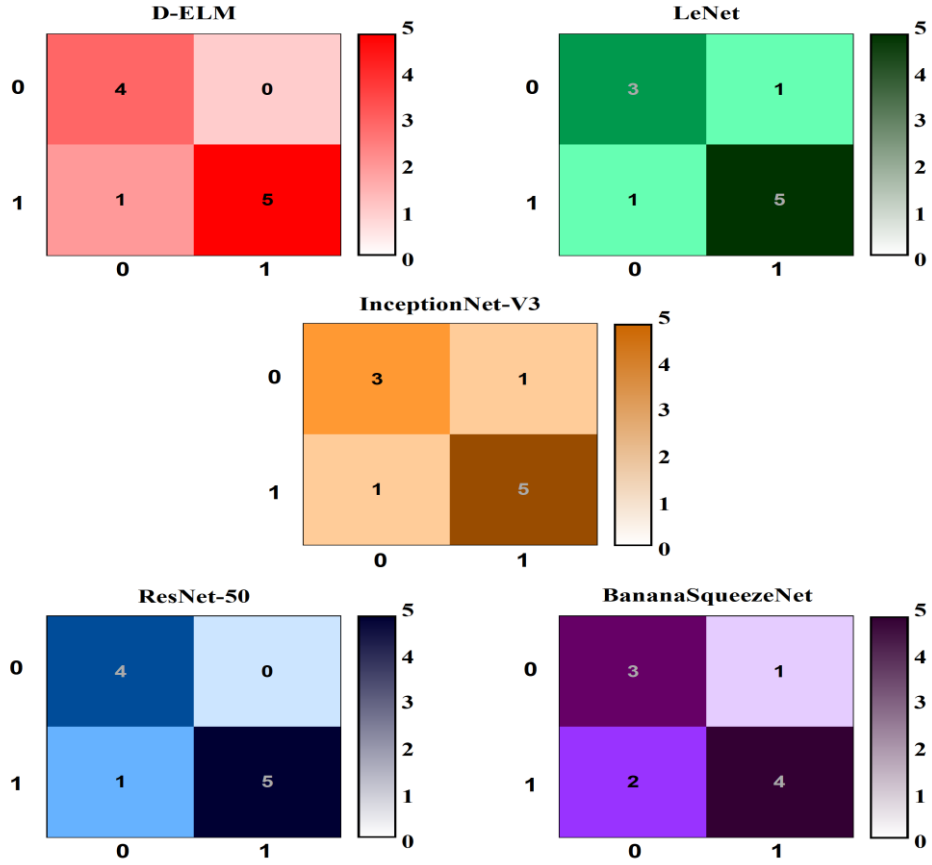

Figure 7. Confusion Matrix

The classification accuracy of the model in terms of its correct classification and misclassification is visually confirmed with the help of the confusion matrix heatmap that demonstrates that D-ELM has a significant number of correct and a limited number of incorrect classifications. This is a clear indication of how effective

the D-ELM model is and the application of CLAHE and contour mathematics can be a massive boost to the model and the extraction of dependable characteristics that are essential in training the model and predicting the diseases. The use of these advanced preprocessing methods has created a new precedence in the future studies in detecting plant disease using these sophisticated artificial intelligence systems.

6. Conclusion And Future Enhancements

The study is a significant improvement to previous studies that did not identify the definite progression of the disease by providing a deep learning model that aimed at classifying the Black Sigatoka disease in banana leaves as per the stages of infection. The approach applied in this research categorize Black Sigatoka stages according to four stages, namely healthy, early, intermediate, and advanced stages. This is unlike in the past where the other studies were largely focused on less comprehensive categorization. Such a comprehensive classification is required to allow specific interventions to be applied in support of illness management approaches. Strengths and Weaknesses: The ease of use and effectiveness of CNN model that yielded an average accuracy of 90 percent in all the stages is an important strength of our methodology. The lightweight nature of this model renders it suitable to be used in resource-constrained applications, e.g., field-use mobile applications. This ease may be problematic, however, because the model may not extend to complex or diverse datasets as the VGG16 model. Even the studies with a 76% precision score showed that VGG16 model was more successful in the generalization.

These shortcomings should be addressed by future studies on hybrid models or deep learning architectures. The interesting thought presented in (21) is that Artificial Neural Networks (ANN) can be used to analyze the health of banana plants; the concept can be further developed to deal with recognizing stages of the Black Sigatoka disease. (22) adopted an ensemble machine learning approach; other parameters during the illness diagnosis and classification can be added on the same concept of ensemble techniques. The study also considered the stem and fruit of bananas in their solution unlike this study. These are other banana products that can be researched in the future.

References

1. Agarap, A. F. (2018). Deep learning using rectified linear units (relu). arXiv preprint arXiv:1803.08375.
2. Almeyda, E., Paiva, J., &Ipanaqué, W. (2020, October). Pest incidence prediction in organic banana crops with machine learning techniques. In 2020 IEEE Engineering International Research Conference (EIRCON) (pp. 1-4). IEEE.
3. Amara, J., Bouaziz, B., &Algergawy, A. (2017). A deep learning-based approach for banana leaf diseases classification. Datenbanksystemefür Business, Technologie und Web (BTW 2017)-Workshopband.
4. Arman E, Shifat; BakiBhuiyan, Md Abdullahil; Abdullah, Hasan Muhammad; Islam, Shariful; Chowdhury, TahsinTanha; Hossain, Md. Arban (2023), "Banana Leaf Spot Diseases (BananaLSD) Dataset for Classification of Banana Leaf Diseases Using Machine Learning", Mendeley Data, V1, doi: 10.17632/9tb7k297ff.1
5. Ashkar, G. P., &Modestino, J. W. (1978). The contour extraction problem with biomedical applications. Computer Graphics and Image Processing, 7(3), 331-355.
6. Bhuiyan, M. A. B., Abdullah, H. M., Arman, S. E., Rahman, S. S., & Al Mahmud, K. (2023). BananaSqueezeNet: A very fast, lightweight convolutional neural network for the diagnosis of three prominent banana leaf diseases. Smart Agricultural Technology, 4, 100214.
7. Burt, P. J., Rosenberg, L. J., Rutter, J., Ramirez, F., & GONZALES O, H. (1999). Forecasting the airborne spread of Mycosphaerellafijiensis, a cause of black Sigatoka disease on banana: estimations of numbers of perithecia and ascospores. Annals of applied biology, 135(1), 369-377.
8. Chaudhari, V., & Patil, M. (2020, August). Banana leaf disease detection using K-means clustering and Feature extraction techniques. In 2020 International Conference on Advances in Computing, Communication & Materials (ICACCM) (pp. 126-130). IEEE.
9. Churchill, A. C. (2011). Mycosphaerellafijiensis, the black leaf streak pathogen of banana: progress towards understanding pathogen biology and detection, disease development, and the challenges of control. Molecular plant pathology, 12(4), 307-328.
10. Haralick, R. M., Shanmugam, K., &Dinstein, I. H. (1973). Textural features for image classification. IEEE Transactions on systems, man, and cybernetics, (6), 610-621.
11. Hu, M. H., Dong, Q. L., Malakar, P. K., Liu, B. L., &Jaganathan, G. K. (2015). Determining banana size based on computer vision. International journal of food properties, 18(3), 508-520.
12. Intaravanne, Y., Sumriddetchkajorn, S., &Nukeaw, J. (2012, May). Ripeness level indication of bananas with visible and fluorescent spectral images. In 2012 9th International Conference on Electrical Engineering/Electronics, Computer, Telecommunications and Information Technology (pp. 1-4). IEEE.
13. Karthick Raghunath, K. M., Koti, M. S., Sivakami, R., Vinoth Kumar, V., NagaJyothi, G., &Muthukumaran, V. (2022). Utilization of IoT-assisted computational strategies in wireless sensor networks for smart infrastructure management. International Journal of System Assurance Engineering and Management, 1-7.
14. Krizhevsky, A., Sutskever, I., & Hinton, G. E. (2017). ImageNet classification with deep convolutional neural networks. Communications of the ACM, 60(6), 84-90.

15. Löfstedt, T., Brynolfsson, P., Asklund, T., Nyholm, T., &Garpebring, A. (2019). Gray-level invariant Haralick texture features. PloS one, 14(2), e0212110.
16. Mduma, N; Laizer, Hudson; Loyani, Loyani; Macheli, Mbwana; Msengi, Zablon; Karama, Alice; Msaki, Irine; Sanga, Sophia; Jomanga, Kennedy; Judith, Leo, 2022, "The Nelson Mandela African Institution of Science and Technology Bananas dataset", https://doi.org/10.7910/DVN/LQUWXW, Harvard Dataverse, V6.
17. Oladejo, B. F., & Ademola, O. O. (2020, July). Automated classification of banana leaf diseases using an optimized capsule network model. In CS & IT Conference Proceedings (Vol. 10, No. 9). CS & IT Conference Proceedings.
18. Olivares, B. O., Vega, A., Rueda Calderón, M. A., Montenegro-Gracia, E., Araya-Almán, M., & Marys, E. (2022). Prediction of banana production using epidemiological parameters of black sigatoka: An application with random forest. Sustainability, 14(21), 14123.
19. Owomugisha, G., Quinn, J. A., Mwebaze, E., &Lwasa, J. (2014, December). Automated vision-based diagnosis of banana bacterial wilt disease and black sigatoka disease. In International conference on the use of mobile ICT in Africa (pp. 1-5).
20. Pandiyan, S., Ashwin, M., Manikandan, R., KM, K. R., & GR, A. R. (2020). Heterogeneous internet of things organization predictive analysis platform for apple leaf diseases recognition. Computer Communications, 154, 99-110.
21. Reza, A. M. (2004). Realization of the contrast limited adaptive histogram equalization (CLAHE) for real-time image enhancement. Journal of VLSI signal processing systems for signal, image and video technology, 38, 35-44.
22. Sanga, S., Mero, V., Machuve, D., &Mwanganda, D. (2020). Mobile-based deep learning models for banana diseases detection. arXiv preprint arXiv:2004.03718.
23. Sebastian V, B., Unnikrishnan, A., & Balakrishnan, K. (2012). Gray level co-occurrence matrices: generalisation and some new features. arXiv preprint arXiv:1205.4831.
24. Sokolova, M., Japkowicz, N., &Szpakowicz, S. (2006, December). Beyond accuracy, F-score and ROC: a family of discriminant measures for performance evaluation. In Australasian joint conference on artificial intelligence (pp. 1015-1021). Berlin, Heidelberg: Springer Berlin Heidelberg.
25. Song, R., Zhang, Z., & Liu, H. (2017). Edge connection based Canny edge detection algorithm. Pattern Recognition and Image Analysis, 27, 740-747.
26. Ugarte Fajardo, J., Bayona Andrade, O., Criollo Bonilla, R., Cevallos-Cevallos, J., Mariduena-Zavala, M., Ochoa Donoso, D., & Vicente Villardon, J. L. (2020). Early detection of black Sigatoka in banana leaves using hyperspectral images. Applications in plant sciences, 8(8), e11383.
27. Ugarte Fajardo, J., Maridueña-Zavala, M., Cevallos-Cevallos, J., & Ochoa Donoso, D. (2022). Effective Methods Based on Distinct Learning Principles for the Analysis of Hyperspectral Images to Detect Black Sigatoka Disease. Plants, 11(19), 2581.
28. Uzair, M., Shafait, F., Ghanem, B., &Mian, A. (2018). Representation learning with deep extreme learning machines for efficient image set classification. Neural Computing and Applications, 30, 1211-1223.
29. Sujatha, R.; Krishnan, S.; Chatterjee, J.M.; Gandomi, A.H. Advancing plant leaf disease detection integrating machine learning and deep learning. Scientific Reports 2025, 15. https://doi.org/10.1038/s41598-024-72197-2.
30. Mora, J.J.; Blomme, G.; Safari, N.; Elayabalan, S.; Selvarajan, R.; Selvaraj, M.G. Digital framework for georeferenced multiplatform surveillance of banana wilt using human in the loop AI and YOLO foundation models. Scientific Reports 2025, 15. https://doi.org/10.1038/s41598-025-87588-2.
31. Batool, A.; Kim, J.; Byun, Y.C. A compact deep learning approach integrating depthwise convolutions andspatial attention for plant disease classification. Plant Methods 2025, 21. https://doi.org/10.1186/s13007-025-01325-4.
32. Bagheri, N.; Kafashan, J. Appropriate vegetation indices and data analysis methods for orchards monitoring using UAV-based remote sensing: A comprehensive research. Computers and Electronics in Agriculture 2025, 235. https://doi.org/10.1016/j.compag.2025.110356.